

Accepted for publication in the  
International Journal of Non-Linear Mechanics

# Resonant Motions of the Three-dimensional Elastic Pendulum

*Peter Lynch*

Met Éireann, Glasnevin Hill, Dublin 9, Ireland

January, 2001

# Resonant Motions of the Three-dimensional Elastic Pendulum

Peter Lynch

Met Éireann, Glasnevin Hill, Dublin 9, Ireland

---

## Abstract

The three-dimensional motion of the elastic pendulum or swinging spring is investigated in this study. The amplitude is assumed to be small, so that the perturbation approach is valid. If the Lagrangian is approximated by keeping terms up to cubic order, the system has three independent constants of motion; it is therefore completely integrable.

The linear normal modes are derived, and some special solutions are considered. For unmodulated motion, with no transfer of energy between vertical and horizontal components, elliptic-parabolic solutions are found, which generalize the solutions first found by Vitt and Gorelik. These solutions are illustrated by numerical integrations. Perturbations about conical motion are then studied, and solutions in terms of elementary functions are found.

When the ratio of the the normal mode frequencies is approximately two to one, an interesting resonance phenomenon occurs, in which energy is transferred periodically between predominantly vertical and predominantly horizontal oscillations. The motion has two distinct characteristic times, that of the oscillations and that of the resonance envelope, and a multiple time-scale analysis is found to be productive. The amplitude of the vertical component may be expressed in terms of Jacobian elliptic functions.

As the oscillations change from horizontal to vertical and back again, it is observed that each horizontal excursion is in a different direction. To study this phenomenon, it is convenient to transform the equations to rotating co-ordinates. Expressions for the precession of the swing-plane are derived. The approximate solutions are compared to numerical integrations of the exact equations, and are found to give a realistic description of the motion.

---

*Keywords:* Elastic Pendulum, Swinging Spring, Nonlinear Resonance, Precession.

# 1 Introduction

The elastic pendulum or swinging spring is a simple mechanical system with highly complex dynamics. It comprises a heavy mass suspended from a fixed point by a light spring which can stretch but not bend, moving under gravity. The state of the system is given by the three spatial co-ordinates of the mass; the system has three degrees of freedom. The equations of motion are easy to write down but, in general, impossible to solve analytically. For finite amplitudes, the motion of the system exhibits chaos, and predictability is severely limited. For small amplitudes, perturbation techniques are valid, the system is integrable, and approximate analytical solutions can be found.

Several studies have considered the chaotic motions of the swinging spring. An extensive list of references may be found in Lynch [15]. The present study is not concerned with the chaotic regime, but with the regular small-amplitude motions of the system. Various perturbation techniques are employed to derive analytical expressions for the motion. These solutions are compared with numerical solutions of the full equations, to illustrate the validity of the approximations.

The linear normal modes of the system are of two distinct types, a vertical or springing oscillation in which elasticity is the restoring force, and quasi-horizontal swinging oscillations in which the system acts like a pendulum. When the frequencies of the springing and swinging modes are in the ratio 2:1, an interesting non-linear resonance phenomenon occurs, in which energy is transferred periodically back and forth between the springing and swinging motions. The earliest substantial study of the elastic pendulum was by Vitt and Gorelik [21]. These authors discussed the resonance phenomenon and also derived some special periodic solutions.

A large number of other papers have been published following Vitt and Gorelik (for example, Refs. [1, 2, 4–10, 13, 14, 17–19]). The contents of these studies are briefly outlined by Lynch [15]. All considered motion confined to two dimensions. As there is no torque about the vertical line through the point of suspension, the angular momentum about this line must be constant. In the case of zero angular momentum, the motion takes place in a plane; there are then only two degrees of freedom. (Cayton [5] briefly discussed three-dimensional solutions, mentioning some numerical difficulties associated with the use of polar co-ordinates, but gave few details).

The present work is concerned with the three-dimensional motion in the case of resonance. In particular, the precession of the swing plane is investigated. If the initial motion is quasi-vertical, the resonance has the consequence that an essentially horizontal swinging motion develops: with small angular momentum, the motion is then approximately planar. This motion is subsequently replaced by springy oscillations similar to the initial motion. When horizontal swinging motion develops again, the plane of swing is in a different direction. This variation between springing and swinging motion continues indefinitely. The change in direction of the swing plane from one horizontal excursion to the next depends critically on the initial conditions. We derive expressions for the angle of precession in terms of these conditions.<sup>1</sup>

The contents of this paper will now be summarized. In §2, the basic equations are set down, and some simple solutions are derived. The linear normal modes are derived, the elastic or springing modes where the motion of the bob is vertical, and the rotational or swinging modes where the motion is quasi-horizontal. In §3 we investigate unmodulated solutions, that is, those for which there is no transfer of energy between the swinging and springing modes. The cup-like and cap-like periodic solutions first found by Vitt and Gorelik [21] are generalized to the case of three dimensions. Solutions are found having horizontal projections which are precessing or retrogressing ellipses.

In §4, perturbations about conical motion are studied. The modulation equations are found to be soluble in terms of elementary functions. In the case of maximal energy transfer, the horizontal projection does not rotate, but each axis of the ellipse alternates between being major and minor. Numerical solutions are presented to illustrate the motion. In §5 general small-amplitude motions are considered, and the multiple time-scale technique is employed. The slowly varying amplitudes and phases of the components of the motion are governed by a system of six equations, the modulation equations. A single equation may be derived for the amplitude of the vertical component, and its solution expressed in terms of Jacobian elliptic functions. Although the system is integrable, it is cumbersome to derive explicit expressions for the remaining variables.

In §6 we consider the general equations in co-ordinates which rotate with an unspecified, time-dependent angular velocity. The purpose is to find an expression for the precession

---

<sup>1</sup>The precession phenomenon bears similarity to the well-known rotation of the plane of oscillation of a Foucault pendulum, but the latter results from the non-inertial frame, and the mechanisms are quite different.

of the solution about the vertical. A set of modulation equations is derived, again using the two-timing technique. The equation for the vertical amplitude is formally identical to that in non-rotating co-ordinates. It can be solved analytically, and the angular velocity of the co-ordinate system may be expressed in terms of the vertical amplitude. We derive approximate expressions for the precession rate, which yield results close to those obtained by numerical integration of the full equations.

## 2 The Dynamic Equations for the Swinging Spring

### 2.1 The Exact Equations of Motion

The physical system to be studied consists of a mass, suspended from a fixed point by a light spring which can stretch but not bend, moving under gravity. The position of the mass is given by its three spatial co-ordinates: the system has three degrees of freedom. As there is no torque about the vertical line through the point of suspension, the angular momentum about this line must be constant. In the case of zero angular momentum, the motion takes place in a plane; there are then only two degrees of freedom.

We present the exact equations in three co-ordinate systems, each having advantages in certain circumstances. Let  $\ell_0$  be the unstretched length of the spring,  $k$  its elasticity or stiffness and  $m$  the mass of the bob. At equilibrium the weight is balanced by the elastic restoring force:

$$k(\ell - \ell_0) = mg. \quad (1)$$

We first consider cartesian co-ordinates  $(x, y, Z)$  centered at the point of suspension of the pendulum. The Lagrangian is

$$L = T - V = \frac{1}{2}m(\dot{x}^2 + \dot{y}^2 + \dot{Z}^2) - \frac{1}{2}k(r - \ell_0)^2 - mgZ \quad (2)$$

where  $r = \sqrt{(x^2 + y^2 + Z^2)}$ . The equations of motion may be written:

$$\ddot{x} = -\omega_Z^2 \left( \frac{r - \ell_0}{r} \right) x \quad (3)$$

$$\ddot{y} = -\omega_Z^2 \left( \frac{r - \ell_0}{r} \right) y \quad (4)$$

$$\ddot{Z} = -\omega_Z^2 \left( \frac{r - \ell_0}{r} \right) Z - g \quad (5)$$

where  $\omega_Z^2 = k/m$ . There are two equilibrium states, where the velocities vanish identically. The first is stable, with the spring hanging vertically downward ( $x = 0, y = 0, Z = -\ell$ ), and the balance of forces is given by (1). The second is an unstable equilibrium with the mass balanced precariously above the point of suspension, at least for  $\ell < 2\ell_0$  ( $x = 0, y = 0, Z = 2\ell_0 - \ell$ ). There are two constants of the motion, the energy  $E = T + V$  and the angular momentum per unit mass,  $h = x\dot{y} - y\dot{x}$ , about the vertical. Since the system has three degrees of freedom and only two invariants, it is not in general integrable.

Next, consider spherical co-ordinates  $(r, \theta, \varphi)$ , with the angle  $\theta$  measured from the downward vertical. The Lagrangian is

$$L = \frac{1}{2}m \left( \dot{r}^2 + (r\dot{\theta})^2 + (r \sin \theta \dot{\varphi})^2 \right) - \frac{1}{2}k(r - \ell_0)^2 + mgr \cos \theta \quad (6)$$

and the equations of motion are

$$\ddot{r} = -\omega_Z^2(r - \ell_0) + g \cos \theta + r\dot{\theta}^2 + r \sin^2 \theta \dot{\varphi}^2 \quad (7)$$

$$\frac{d}{dt}(r^2\dot{\theta}) = -gr \sin \theta + r^2 \sin \theta \cos \theta \dot{\varphi}^2 \quad (8)$$

$$\frac{d}{dt}(r^2 \sin^2 \theta \dot{\varphi}) = 0 \quad (9)$$

Finally, we may express the Lagrangian in cylindrical co-ordinates as

$$L = \frac{1}{2}m \left( \dot{R}^2 + (R\dot{\varphi})^2 + \dot{Z}^2 \right) - \frac{1}{2}k(r - \ell_0)^2 - mgZ \quad (10)$$

where  $r = \sqrt{(R^2 + Z^2)}$ . The equations of motion are

$$\ddot{R} = -\omega_Z^2 \left( \frac{r - \ell_0}{r} \right) R + R\dot{\varphi}^2 \quad (11)$$

$$\ddot{Z} = -\omega_Z^2 \left( \frac{r - \ell_0}{r} \right) Z - g \quad (12)$$

$$\frac{d}{dt}(R^2\dot{\varphi}) = 0 \quad (13)$$

## 2.2 Linear Normal Modes

With cartesian co-ordinates, it is convenient for analysis of small amplitude motions to move the origin to the point of stable equilibrium; the vertical co-ordinate is then  $z = Z + \ell$ . We can simplify the equations, supposing that the amplitude of the motion is

small,  $|x| \ll \ell$ ,  $|y| \ll \ell$  and  $|z| = |Z + \ell| \ll \ell$  and using (1). Keeping only linear terms, equations (3) and (4) become

$$\ddot{x} + \omega_R^2 x = 0, \quad \ddot{y} + \omega_R^2 y = 0. \quad (14)$$

where  $\omega_R = \sqrt{g/\ell}$  is the frequency of a linear simple (anelastic) pendulum. The solutions may be written immediately in the form

$$x = a \cos(\omega_R t) + b \sin(\omega_R t), \quad y = c \cos(\omega_R t) + d \sin(\omega_R t).$$

Thus, the horizontal projection of the motion, in the limit of small amplitudes, is an ellipse centered at the origin, traversed with frequency  $\omega_R$ . The linear vertical motion is given by simplifying (5) to get

$$\ddot{z} + \omega_Z^2 z = 0, \quad (15)$$

the equation for elastic oscillations with frequency  $\omega_Z = \sqrt{k/m}$ . We call the motion described by (14) the rotational component and that described by (15) the elastic component. In the linear limit, there is no interaction between them. We introduce the ratio of the rotational and elastic frequencies:

$$\epsilon \equiv \left( \frac{\omega_R}{\omega_Z} \right) = \sqrt{\frac{mg}{k\ell}}.$$

It follows from (1) that the rotational frequency is always less than the elastic:

$$\epsilon^2 = \left( 1 - \frac{\ell_0}{\ell} \right) < 1, \quad \text{so that} \quad |\omega_R| < |\omega_Z|.$$

If the frequencies are commensurate, i.e., if  $\epsilon$  is a rational number, the linear motion is periodic. If  $\epsilon$  is irrational, the variables never return simultaneously to their starting values, but come arbitrarily close; the motion is then said to be quasi-periodic.

## 2.3 Conical Motion

We consider next the case of conical motion, with  $r$ ,  $\theta$  and  $\dot{\varphi} = \omega$  all constant. Spherical co-ordinates are most convenient. The equations of motion (7)–(9) reduce to

$$r\omega^2 \sin^2 \theta - \omega_Z^2(r - \ell_0) + g \cos \theta = 0 \quad (16)$$

$$r\omega^2 \cos \theta - g = 0 \quad (17)$$

$$r^2 \omega \sin^2 \theta = h \quad (18)$$

From the first two we can easily derive the relationship for the spring length in terms of the conic angle:

$$r = \ell_0 + \frac{g}{\omega_Z^2 \cos \theta} \quad (19)$$

This relationship is of the form  $r = a + b \sec \theta$ , which is the standard form of the equation of a *conchoid*. This special curve was used by the Greek mathematician Nicomedes (c. 200 B.C.) to devise methods of tri-secting angles and duplicating the cube (see, e.g., [3], p727).

Noting that  $Z = -r \cos \theta$  and  $g/\omega_Z^2 = \epsilon^2 \ell$ , it follows that

$$Z = -\epsilon^2 \ell - \ell_0 \cos \theta$$

so that, for  $|\theta| < \pi/2$ ,  $Z$  is bounded above by a value less than zero: for conical motion, the bob cannot be above the plane  $Z = -\epsilon^2 \ell$ . The relationship between  $Z$  and  $R$  is

$$(Z + b)^2(Z^2 + R^2) - a^2 Z^2 = 0$$

(with  $a = \ell_0$ ,  $b = \epsilon^2 \ell$ ). Although this equation is more complicated than (19), it gives the limiting cases easily:  $Z = -\ell$  when  $R = 0$  and  $Z \rightarrow -\epsilon^2 \ell$  as  $R \rightarrow \infty$ .

From (12) and (17), the angular velocity is given by

$$\omega^2 = \frac{g}{r \cos \theta} = \left( \frac{r - \ell_0}{r} \right) \omega_Z^2$$

As  $\theta \rightarrow 0$ ,  $\omega$  tends to  $\omega_R$ , and as  $R \rightarrow \infty$ ,  $\omega$  tends to  $\omega_Z$ . This is a curiosity, distinct from the behaviour of the simple or anelastic conical pendulum, where the angular velocity may take arbitrarily large values. The higher energy states of the spring pendulum are possible with bounded  $\omega$ , as the extension  $r$  may increase without limit, allowing  $E$  and  $h$  to become arbitrarily large.

### 3 Unmodulated Solutions

#### 3.1 Cup and Cap Modes

We next discuss unmodulated solutions, where there is no energy exchange between the elastic and pendular motions. Starting from the Lagrangian (2), keeping only terms up to cubic order, assuming  $m = 1$  and dropping an irrelevant constant term, we get

$$L = \frac{1}{2}[\dot{x}^2 + \dot{y}^2 + \dot{z}^2] - \frac{1}{2}[\omega_R^2(x^2 + y^2) + \omega_Z^2 z^2] + \frac{1}{2}\lambda(x^2 + y^2)z \quad (20)$$

where  $\lambda = \ell_0 \omega_Z^2 / \ell^2$ . The simplest steady-state motions occur in the special case where  $\omega_Z = 2\omega_R$ ; we assume this to be the case. First, let us consider motion in the  $x$ - $z$ -plane. The equations in rectangular co-ordinates for small amplitude motion are

$$\ddot{x} + \omega_R^2 x = \lambda x z \quad (21)$$

$$\ddot{z} + 4\omega_R^2 z = \frac{1}{2} \lambda x^2 \quad (22)$$

and we seek solutions which at lowest order have simple periodic form:

$$x = \epsilon(A \cos \omega t) + \epsilon^2 x_2 + \dots \quad (23)$$

$$z = \epsilon(C \cos 2\omega t) + \epsilon^2 z_2 + \dots \quad (24)$$

where  $A$  and  $C$  are constants and  $\omega = \omega_0 + \epsilon\omega_1 + \dots$  is to be determined. The  $O(\epsilon)$  equations imply  $\omega_0 = \omega_R$  and give the lowest-order terms  $x_1 = A \cos \omega_R t$  and  $z_1 = C \cos 2\omega_R t$ . The  $O(\epsilon^2)$  equations are then

$$\ddot{x}_2 + \omega_R^2 x_2 = 2\omega_R \omega_1 A \cdot \cos \omega_R t + \lambda A C \cdot \cos \omega_R t \cos 2\omega_R t$$

$$\ddot{z}_2 + 4\omega_R^2 z_2 = 8\omega_R \omega_1 C \cdot \cos 2\omega_R t + \frac{1}{2} \lambda A^2 \cdot \cos^2 \omega_R t$$

To avoid resonance, the secular terms on the right-hand side must vanish, which results in the relationships

$$2\omega_R \omega_1 A + \frac{1}{2} \lambda A C = 0 \quad (25)$$

$$8\omega_R \omega_1 C + \frac{1}{4} \lambda A^2 = 0 \quad (26)$$

We have two equations for three unknowns,  $A$ ,  $C$  and  $\omega_1$ . Fixing the horizontal amplitude  $A$ , it follows that

$$C = \pm \left( \frac{A}{2\sqrt{2}} \right), \quad \omega_1 = \mp \left( \frac{3\sqrt{2}A}{16\ell} \right) \omega_R \quad (27)$$

There are thus two solutions, depending on the choice of sign. Taking the upper signs in (27) we have the solutions

$$z = + \frac{A}{\sqrt{2}} \left[ \left( \frac{x}{A} \right)^2 - \frac{1}{2} \right], \quad \omega = \omega_R \left( 1 - \frac{3\sqrt{2}A}{16\ell} \right)$$

The trajectory is an upright or cup-like parabola and the frequency is diminished slightly relative to  $\omega_R$ . The lower signs in (27) give the solution

$$z = - \frac{A}{\sqrt{2}} \left[ \left( \frac{x}{A} \right)^2 - \frac{1}{2} \right], \quad \omega = \omega_R \left( 1 + \frac{3\sqrt{2}A}{16\ell} \right)$$

which has an inverted or cap-like trajectory and a slightly augmented frequency. These parabolic steady solutions were first derived by Vitt and Gorelik [21]. They can be easily demonstrated with a physical spring pendulum by drawing the bob to one side and trying various points of release. A third solution of (25)–(26), with  $A = \omega_1 = 0$  and arbitrary  $C$ , corresponds to purely vertical oscillations, which however are unstable.

### 3.2 Elliptic-Parabolic Modes

We look next at the three-dimensional case. The small-amplitude equations corresponding to the Lagrangian (20) are

$$\ddot{x} + \omega_R^2 x = \lambda x z \quad (28)$$

$$\ddot{y} + \omega_R^2 y = \lambda y z \quad (29)$$

$$\ddot{z} + 4\omega_R^2 z = \frac{1}{2}\lambda(x^2 + y^2) \quad (30)$$

If we seek solutions which at lowest order have simple periodic form

$$x = \epsilon(A \cos \omega t) + \epsilon^2 x_2 + \dots \quad (31)$$

$$y = \epsilon(B \sin \omega t) + \epsilon^2 y_2 + \dots \quad (32)$$

$$z = \epsilon(C \cos 2\omega t) + \epsilon^2 z_2 + \dots \quad (33)$$

where  $A$ ,  $B$  and  $C$  are constants and  $\omega = \omega_0 + \epsilon\omega_1 + \dots$ , the requirement that secular terms in the second-order equations vanish leads to the conditions

$$2\omega_R\omega_1 A + \frac{1}{2}\lambda AC = 0$$

$$2\omega_R\omega_1 B - \frac{1}{2}\lambda BC = 0$$

$$8\omega_R\omega_1 C + \frac{1}{4}\lambda(A^2 - B^2) = 0$$

We have three equations for four unknowns,  $A$ ,  $B$ ,  $C$  and  $\omega_1$ . If  $A = 0$  or  $B = 0$  we have the cup-like and cap-like solutions. For  $C = 0$  we have conical motion (with  $A = B$  and  $\omega_1 = 0$ ). For  $ABC \neq 0$  there are no solutions to these equations.

We seek more general solutions by transforming the equations to rotating co-ordinates

$$\begin{pmatrix} \xi \\ \eta \\ \zeta \end{pmatrix} = \begin{pmatrix} \cos \Theta & \sin \Theta & 0 \\ -\sin \Theta & \cos \Theta & 0 \\ 0 & 0 & 1 \end{pmatrix} \begin{pmatrix} x \\ y \\ z \end{pmatrix}$$

where  $\Theta$  may vary with time. If we assume the  $(\xi - \eta)$  axes rotate with constant angular velocity  $\dot{\Theta} = \Omega$ , the equations become

$$\ddot{\xi} + (\omega_R^2 - \Omega^2)\xi - 2\Omega\dot{\eta} = \lambda\xi\zeta$$

$$\ddot{\eta} + (\omega_R^2 - \Omega^2)\eta + 2\Omega\dot{\xi} = \lambda\eta\zeta$$

$$\ddot{\zeta} + 4\omega_R^2\zeta = \frac{1}{2}\lambda(\xi^2 + \eta^2)$$

These differ from (28)–(30) in two respects: the frequency  $\omega_R^2$  in the horizontal equations is modified to become  $(\omega_R^2 - \Omega^2)$ , and there are additional Coriolis terms  $(-2\Omega\dot{\eta}, +2\Omega\dot{\xi})$  in these equations. We seek solutions of the form

$$\xi = \epsilon(A \cos \omega t) + \epsilon^2 \xi_2 + \dots \quad (34)$$

$$\eta = \epsilon(B \sin \omega t) + \epsilon^2 \eta_2 + \dots \quad (35)$$

$$\zeta = \epsilon(C \cos 2\omega t) + \epsilon^2 \zeta_2 + \dots \quad (36)$$

We now assume that the rotation is small:  $\Omega = \epsilon\Omega_1$ . Then the first-order equations do not contain  $\Omega$ , imply  $\omega_0 = \omega_R$  and yield the solutions

$$\xi_1 = A \cos \omega_R t \quad , \quad \eta_1 = B \sin \omega_R t \quad , \quad \zeta_1 = C \cos 2\omega_R t$$

The motion is elliptic in its horizontal projection and the  $\xi$ – $\zeta$  and  $\eta$ – $\zeta$  projections are parabolic, one cup-like and one cap-like. The requirement that the secular terms in the second-order equations vanish leads to the conditions

$$2\omega_R\omega_1 A + \frac{1}{2}\lambda AC + 2\Omega_1\omega_R B = 0$$

$$2\omega_R\omega_1 B - \frac{1}{2}\lambda BC + 2\Omega_1\omega_R A = 0$$

$$8\omega_R\omega_1 C + \frac{1}{4}\lambda(A^2 - B^2) = 0$$

These are straightforward to solve for given values of  $A$  and  $B$ :

$$C = \pm \frac{A^2 - B^2}{2\sqrt{2(A^2 + B^2)}}, \quad (37)$$

$$\omega_1 = \mp \left( \frac{3\sqrt{2(A^2 + B^2)}}{16\ell} \right) \omega_R, \quad (38)$$

$$\Omega_1 = \pm \left( \frac{3AB}{4\ell\sqrt{2(A^2 + B^2)}} \right) \omega_R. \quad (39)$$

We note that  $|\Omega_1/\omega_1| = 2AB/(A^2 + B^2) \leq 1$ , with equality for a circular orbit.

### 3.3 Numerical Examples

To illustrate the nature of the elliptic-parabolic modes, we present the results of some numerical integrations of the exact equations (3)–(5). The parameter values are  $m = 1$  kg,  $\ell = 1$  m,  $g = \pi^2 \text{ m s}^{-2}$  and  $k = 4\pi^2 \text{ kg s}^{-2}$  so that  $\epsilon = \frac{1}{2}$ ,  $\omega_R = \pi$ ,  $\omega_Z = 2\pi$ . The linear rotational mode has period  $\tau_R = 2$  s, and the vertical mode has half this period,  $\tau_Z = 1$  s. These values will be used for all numerical integrations unless otherwise indicated.

We select the initial conditions by specifying the semi-axes major and minor:  $A = 0.01$  and  $B = 0.005$ , representing an ellipse of eccentricity 0.866. The amplitude is kept small so that the approximations made above are reasonably accurate. The amplitude  $C$  is given by (37). We first choose the upper signs. The initial position and velocity are  $(x, y, z) = (A, 0, C)$  and  $(\dot{x}, \dot{y}, \dot{z}) = (0, \omega B, 0)$ , where  $\omega = \omega_R + \omega_1$  with  $\omega_1$  given by (38). Initially, the elliptical motion is oriented with the major axis in the  $x$ -direction. The precession rate  $\Omega_1$  is given by (39) and, for the given initial conditions, has the value  $\Omega_1 = 0.00745$ , which implies a precession of  $90^\circ$  in 211 seconds.

We show the horizontal projection of the motion in Fig. 1(top). The trajectory is indeed an ellipse which rotates in the sense of the motion, and the angle of precession over the 211 second duration of the integration is very close to  $90^\circ$ , the value predicted by (39). The amplitude of the elliptical horizontal motion is sensibly constant. In Fig. 1 (bottom panel) we show  $z$  plotted against  $R$ . It is seen that the trajectory in this projection is confined to a narrow strip, corresponding closely to the theoretical cup-shaped parabola.

In Fig. 2 the solution corresponding to the lower signs in (37)–(39) is shown. Again the horizontal projection is elliptical in character, but this time it is retrogressive, as expected. That is, the sense of precession of the ellipse is clockwise, opposite to the anti-clockwise rotation of the bob about the vertical. The vertical projection  $z$  versus  $R$  is again confined to a narrow strip, now cap-like as predicted by theory. For both solutions, the rotational and elastic components of the energy were examined (not shown) and were found to be substantially constant.

## 4 Near-Conical Motions

We now investigate motions near to steady conical motion, using the method of harmonic balance (Jordan and Smith [10]). This method requires a certain sleight of hand to apply,

and can appear somewhat cavalier. Indeed, Kahn [11] illustrates some of its deficiencies and remarks that it should be used with caution. However, it has the great appeal of simplicity and the results below have been confirmed to be consistent with those obtained using the more transparent, if also more cumbersome, method of multiple time scales.

#### 4.1 The Method of Harmonic Balance

We assume as before that  $\omega_Z = 2\omega_R$ . Keeping terms to cubic order and using cylindrical co-ordinates with  $z = Z + \ell$ , the Lagrangian has the form

$$L = \frac{1}{2}(\dot{R}^2 + (R\dot{\phi})^2 + \dot{z}^2) - \frac{1}{2}(\omega_R^2 R^2 + \omega_Z^2 z^2) + \frac{1}{2}\lambda R^2 z \quad (40)$$

where  $\lambda = \ell_0 \omega_Z^2 / \ell^2 = 3\omega_R^2 / \ell$  and we assume  $m = 1$ . So, the equations of motion are

$$\ddot{R} + \omega_R^2 R = \lambda R z + R\dot{\phi}^2 \quad (41)$$

$$\ddot{z} + \omega_Z^2 z = \frac{1}{2}\lambda R^2 \quad (42)$$

$$R^2 \dot{\phi} = h \quad (43)$$

where  $h$  is the (constant) angular momentum per unit mass. First, we consider the basic state with  $\ddot{R} = \ddot{z} = 0$  and  $\dot{\phi} = \omega_0$ , constant. Neglecting a small term  $\lambda R z$  in (41) we find, from (41) and (42) respectively, that

$$R_0 = \sqrt{\frac{h_0}{\omega_R}} \quad ; \quad z_0 = \frac{\lambda R_0^2}{8\omega_R^2} = \frac{3}{8} \left( \frac{R_0}{\ell} \right) R_0. \quad (44)$$

Note that since  $R_0 \ll \ell$ , we have  $z_0 \ll R_0$ . The basic state is one of conical motion. For elliptical motion, if  $x$  and  $y$  vary with frequency  $\omega_R$  then  $R$  goes as  $2\omega_R = \omega_Z$ . So, let us seek solutions of the form

$$R = R_0 + S(t) \cos(\omega_Z t + \sigma(t)) \quad (45)$$

$$z = z_0 + C(t) \cos(\omega_Z t + \gamma(t)) \quad (46)$$

We assume that  $S(t), C(t), \sigma(t)$  and  $\gamma(t)$  are slowly varying, and that  $S, C$  and  $z_0$  are small compared to  $R_0$ . We substitute these solutions into (41) and (42) and neglect small terms to get

$$\begin{aligned} -2\omega_Z \dot{S} \sin(\omega_Z t + \sigma) - 2\omega_Z S \dot{\sigma} \cos(\omega_Z t + \sigma) = \\ \lambda R_0 C \sin(\sigma - \gamma) \sin(\omega_Z t + \sigma) + \lambda R_0 C \cos(\sigma - \gamma) \cos(\omega_Z t + \sigma) \\ -2\omega_Z \dot{C} \sin(\omega_Z t + \gamma) - 2\omega_Z C \dot{\gamma} \cos(\omega_Z t + \gamma) = \\ -\lambda R_0 S \sin(\sigma - \gamma) \sin(\omega_Z t + \gamma) + \lambda R_0 S \cos(\sigma - \gamma) \cos(\omega_Z t + \gamma) \end{aligned}$$

Now we apply the method of harmonic balance, equating the coefficients of the rapidly varying sine and cosine terms. The resulting ‘modulation equations’ are:

$$\dot{S} = -\nu C \sin(\sigma - \gamma) \quad (47)$$

$$\dot{C} = +\nu S \sin(\sigma - \gamma) \quad (48)$$

$$S\dot{\sigma} = -\nu C \cos(\sigma - \gamma) \quad (49)$$

$$C\dot{\gamma} = -\nu S \cos(\sigma - \gamma) \quad (50)$$

where  $\nu = \lambda R_0 / 2\omega_Z$ . As we will soon see, these equations are soluble in terms of elementary functions. First we easily verify that

$$N^2 = S^2 + C^2 \quad \text{and} \quad H = SC \cos(\sigma - \gamma)$$

are constants of the motion. The quantity  $N^2$  is an average of energies in the horizontal and vertical deviations from conical motion. It is easily shown that the quantity  $\nu H$  is the Hamiltonian for the generalized co-ordinates  $(\frac{1}{2}S^2, \frac{1}{2}C^2)$  and conjugate momenta  $(\sigma, \gamma)$ . Since angular momentum  $h$  is also conserved, we have three independent constants and the motion is completely integrable.

We now derive a single equation for  $C$ . Differentiating (48) and using the other modulation equations to eliminate the remaining variables, we get

$$\frac{d^2 C}{d\tau^2} + C = \frac{H^2}{C^3}$$

where the time has been rescaled to  $\tau = \nu t$ . This is isomorphic to the equation of motion under a central force varying in proportion to distance (see, e.g., [20], p156) but here the independent variable is time rather than azimuthal angle. We can write a first integral immediately:

$$\frac{1}{2} \left( \frac{dC}{d\tau} \right)^2 + \frac{1}{2} \left( C^2 + \frac{H^2}{C^2} \right) = E$$

where  $E$  is constant. This is formally the energy equation for a particle moving in a potential field varying as  $V(C) = \frac{1}{2}(C^2 + H^2/C^2)$ . It is easily integrated, but we will obtain our solution more simply by introducing the variables  $\Sigma = S \exp(i\sigma)$  and  $\Xi = C \exp(i\gamma)$ . The modulation equations (47)–(50) then become  $\Sigma' = -i\Xi$  and  $\Xi' = -i\Sigma$ , where primes denote  $\tau$ -derivatives, and the new variables are governed by

$$\Sigma'' + \Sigma = 0 \quad , \quad \Xi'' + \Xi = 0 .$$

The solutions of these equations are

$$\Sigma(\tau) = \Sigma(0) \cos \tau + \Sigma'(0) \sin \tau \quad (51)$$

$$\Xi(\tau) = \Xi(0) \cos \tau + \Xi'(0) \sin \tau \quad (52)$$

Noting that  $R - R_0 = \Re[\Sigma \cdot \exp(i\omega_Z t)]$  and  $z - z_0 = \Re[\Xi \cdot \exp(i\omega_Z t)]$ , it follows that

$$R = R_0 + S_0 \cos \nu t \cdot \cos(\omega_Z t + \sigma_0) + C_0 \sin \nu t \cdot \sin(\omega_Z t + \gamma_0) \quad (53)$$

$$z = z_0 + C_0 \cos \nu t \cdot \cos(\omega_Z t + \gamma_0) + S_0 \sin \nu t \cdot \sin(\omega_Z t + \sigma_0) \quad (54)$$

where  $S_0, C_0, \sigma_0$  and  $\gamma_0$  are initial values. The perturbed motion is thus a fast oscillation, of frequency  $\omega_Z$ , modulated by an envelope of low frequency. The modulation frequency  $\nu = \lambda R_0 / 2\omega_Z$  depends only on fixed system parameters and on the radius  $R_0$  of the basic state of conical motion.

We consider two special cases. First, assume all the perturbation energy is in the horizontal motion. So,  $z(0) = z_0$  and  $C_0 = 0$ . Then

$$R = R_0 + S_0 \cos \nu t \cdot \cos(\omega_Z t + \sigma_0) \quad (55)$$

$$z = z_0 + S_0 \sin \nu t \cdot \sin(\omega_Z t + \sigma_0). \quad (56)$$

The envelopes of the radial and vertical motions vary sinusoidally, with complete transfer of perturbation energy back and forth. The period of the modulation envelop is  $2\pi/\nu$ ; the period of the modulation itself is half this value:  $\tau_M = \pi/\nu$ .

To first order, the horizontal motion is in an ellipse. The time for one cycle (two maxima of  $R$ ) is  $\tau_R = 4\pi/\omega_Z$ . Let angle brackets denote an average over this time. To first order,  $\langle R \rangle = R_0$ ,  $\langle R^2 \rangle = R_0^2$  and  $\langle \dot{\varphi} \rangle = \omega_R$ . Thus, the angular change in one cycle is

$$\Delta\varphi(\tau_R) = \int_0^{\tau_R} \dot{\varphi} dt = \tau_R \omega_R = 2\pi$$

and there is no precession of the ellipse at at this order of approximation (this is confirmed by the numerical example below).

The second special case is  $C_0 = S_0$  and  $\sigma_0 = \gamma_0 = 0$ . The solution is

$$R = R_0 + S_0 \cos[(\omega_Z - \nu)t] \quad (57)$$

$$z = z_0 + S_0 \cos[(\omega_Z - \nu)t]. \quad (58)$$

This is an unmodulated solution of sinusoidal form. The frequency is slightly diminished. The horizontal radius varies between maximum  $a = R_0 + S_0$  and minimum  $b = R_0 - S_0$ , in an approximately elliptical trajectory. Consider the time for  $R$  to pass from a maximum  $a$  through two more maxima:

$$\tau = \frac{4\pi}{\omega_Z - \nu} \approx \tau_R (1 + \eta) ,$$

where  $\eta = \nu/\omega_Z$ . But, as before,  $\langle R^2 \rangle = R_0^2$  and  $\langle \dot{\varphi} \rangle = \omega_R$ , so

$$\Delta\varphi(\tau) = \int_0^\tau \dot{\varphi} dt = \tau\omega_R \approx 2\pi (1 + \eta) .$$

Thus, the ellipse turns through an angle  $2\pi\eta$  in time  $\tau$  so its precession rate is

$$\Omega = \frac{2\pi\eta}{\tau} \approx \eta\omega_R = \frac{\lambda R_0}{4\omega_Z} .$$

This is a particular example of the unmodulated elliptic-parabolic motion discussed in §3.2. The case  $C_0 = -S_0$  and  $\sigma_0 = \gamma_0 = 0$  corresponds to a retrogressing ellipse with  $\omega = \omega_Z + \nu$  and  $\Omega = -\eta\omega_R$ .

## 4.2 A Numerical Example

We illustrate the near-conical perturbation motion in Figs. 3 and 4. The spring parameters are as before. The conical motion is established by choosing the initial position  $x_0 = 0.04$ ,  $y_0 = 0$  and  $z_0 = +3x_0^2/8\ell = 0.0006$  (based on (44)) and the initial velocity  $\dot{x}_0 = \dot{z}_0 = 0$  and  $\dot{y}_0 = \omega_R x_0 = 0.12566$ . The resulting integration is not shown, as it is a simple conical motion with no variation in the vertical component.

We now impose a small perturbation on the vertical velocity,  $\dot{z}_0 = \frac{1}{2}\dot{y}_0 = 0.06283$ . We show the horizontal projection of the motion in Fig. 3(top). The orbit varies from circular to elliptical and back, without any evidence of precession. In Fig. 3 (bottom panel) we show  $z$  plotted against  $R$ . It is seen that, in contrast to the solutions shown in Figs. 1 and 2, this projection is no longer confined to a narrow strip, but fills a diamond-shaped area.

In Fig. 4 the radial distance  $R$  is plotted against time for the 100s duration of the integration. It executes three modulations about its mean value. In the lower panel, the variation of the eccentricity (calculated from the ratio of maximum and minimum  $R$  over a period  $\tau_R$ ) is shown. Again, it is clear that there are three elliptical excursions from the circular motion. The theoretical period of modulation is  $\tau_M = \pi/\nu = 33.3$  s. It is clear from the figures that the value for the numerical solution is close to this.

## 5 General Small-Amplitude Perturbations

### 5.1 Modulation Equations in Fixed Co-ordinates

We consider now the general case of small perturbation motion. Let the parameter  $\epsilon$  represent the characteristic amplitude. Assuming small-amplitude motions, the Lagrangian is given by (20) and the equations may be written

$$\begin{aligned}\ddot{x} + \omega_R^2 x &= \lambda x z \\ \ddot{y} + \omega_R^2 y &= \lambda y z \\ \ddot{z} + \omega_Z^2 z &= \frac{1}{2}\lambda(x^2 + y^2)\end{aligned}$$

We will use the technique of two-timing, or the method of multiple time scales (Nayfeh [16], Ch. 6). We assume there are two time scales, a fast time  $t_0 = t$  and a slow time  $t_1 = \epsilon t$ . We expand the solutions in  $\epsilon$ :

$$x = \epsilon x_1(t_0, t_1) + \epsilon^2 x_2(t_0, t_1) + \dots \quad (59)$$

$$y = \epsilon y_1(t_0, t_1) + \epsilon^2 y_2(t_0, t_1) + \dots \quad (60)$$

$$z = \epsilon z_1(t_0, t_1) + \epsilon^2 z_2(t_0, t_1) + \dots \quad (61)$$

Time derivatives depend on both time scales:

$$\frac{d}{dt} = \frac{\partial}{\partial t_0} + \epsilon \frac{\partial}{\partial t_1} = D_0 + \epsilon D_1.$$

The lowest order solutions are

$$x_1 = A(t_1) \cos[\omega_R t_0 + \alpha(t_1)] \quad (62)$$

$$y_1 = B(t_1) \cos[\omega_R t_0 + \beta(t_1)] \quad (63)$$

$$z_1 = C(t_1) \cos[\omega_Z t_0 + \gamma(t_1)] \quad (64)$$

where the amplitudes and phases depend only on the slow time. The second-order equations are

$$D_0^2 x_2 + \omega_R^2 x_2 = [-2D_0 D_1 x_1 + \lambda x_1 z_1] \equiv R_x \quad (65)$$

$$D_0^2 y_2 + \omega_R^2 y_2 = [-2D_0 D_1 y_1 + \lambda y_1 z_1] \equiv R_y \quad (66)$$

$$D_0^2 z_2 + \omega_Z^2 z_2 = \left[-2D_0 D_1 z_1 + \frac{1}{2}\lambda(x_1^2 + y_1^2)\right] \equiv R_z \quad (67)$$

After some algebraic manipulation, using the assumption that  $\omega_Z = 2\omega_R$ , we find that the requirement that the secular forcing terms vanish results in the following modulation equations (dots denote  $t_1$ -derivatives):

$$\dot{A} = -\kappa AC \sin(2\alpha - \gamma) \quad (68)$$

$$\dot{B} = -\kappa BC \sin(2\beta - \gamma) \quad (69)$$

$$\dot{C} = +\frac{1}{4}\kappa[A^2 \sin(2\alpha - \gamma) + B^2 \sin(2\beta - \gamma)] \quad (70)$$

$$\dot{\alpha} = -\kappa C \cos(2\alpha - \gamma) \quad (71)$$

$$\dot{\beta} = -\kappa C \cos(2\beta - \gamma) \quad (72)$$

$$\dot{\gamma} = -\frac{1}{4}\kappa[(A^2/C) \cos(2\alpha - \gamma) + (B^2/C) \cos(2\beta - \gamma)] \quad (73)$$

where  $\kappa = \lambda/4\omega_R$ . Notice that, if  $B \equiv 0$ , this system reduces to the set of equations for planar motion given, for example, in [16], p.264.

## 5.2 Solution of the Perturbation Equation for C

The system (68)–(73) has three constants of motion:

$$\begin{aligned} N^2 &= A^2 + B^2 + 4C^2 \\ H &= [A^2 C \cos(2\alpha - \gamma) + B^2 C \cos(2\beta - \gamma)] \\ J &= AB \sin(\alpha - \beta). \end{aligned}$$

This is easily demonstrated by differentiating and using the modulation equations. Both  $N^2$  and  $H$  are energy variables and  $\omega_R J$  is the averaged angular momentum. ( $N^2$  is the  $O(\epsilon^2)$  part of the mean potential energy and  $H$  is the  $O(\epsilon^3)$  part; it can be shown that  $\kappa H$  is the Hamiltonian of the time-averaged motion, with generalized co-ordinates  $q = (A^2, B^2, 2C^2)$  and conjugate momenta  $p = (\alpha, \beta, \gamma)$ .)

We can derive a single equation for  $C$  by squaring (70) and using the constants of motion to eliminate the other variables. We get

$$\dot{C}^2 = \left(\frac{\kappa}{4}\right)^2 \left[ (4C^2 - N^2)^2 - \frac{H^2}{C^2} - 4J^2 \right]. \quad (74)$$

We can reduce this to a standard form by cross multiplication by  $C^2$ . If we introduce the new dependent variable  $u = 4C^2/N^2$  and rescale the time by  $\tau = \kappa N t$ , we get

$$\frac{1}{2} \left( \frac{du}{d\tau} \right)^2 + V(u) = E \quad (75)$$

where  $\mathcal{J} = 2J/N^2$ ,  $E = -2H^2/N^6$  and the potential  $V$  is given by

$$V(u) = -\frac{1}{2} [u^3 - 2u^2 + u(1 - \mathcal{J}^2)] .$$

We note that  $V(u)$  has three zeros,  $u = 0$ ,  $u = 1 - \mathcal{J}$  and  $u = 1 + \mathcal{J}$ . Eq. (75) is isomorphic to the energy equation of a particle of unit mass, with position  $u$  and energy  $E$ , moving in a potential field  $V(u)$ .

By definition,  $E \leq 0$  and  $0 \leq u \leq 1$ . It is easily shown that  $-1 \leq \mathcal{J} \leq +1$ . In Fig. 5 (top panel) we plot  $V(u)$  for a range of values of  $\mathcal{J}$ . From the form of the potential, we see that (75) can be written

$$\left(\frac{du}{d\tau}\right)^2 = (u - u_1)(u - u_2)(u - u_3) \quad (76)$$

where  $0 \leq u_1 \leq u_2 \leq 1 \leq u_3$  (with equality in limiting cases).

We first consider the special case with  $\mathcal{J} = 0$  and  $E = 0$ . There is an unstable equilibrium at  $u = 1$ , corresponding to purely vertical oscillations of the spring. The equation (76) reduces to

$$\left(\frac{du}{d\tau}\right)^2 = u(u - 1)^2 \quad (77)$$

which has the solution  $u = \tanh^2[\frac{1}{2}(\tau - \tau_0)]$ . This leads to

$$C = \frac{1}{2}N \tanh[\frac{1}{2}\kappa N(t - t_0)] , \quad S = N \operatorname{sech}[\frac{1}{2}\kappa N(t - t_0)] \quad (78)$$

where  $S^2 = A^2 + B^2$ . Whatever the starting point, all the energy eventually transfers to the springing motion, but the process takes forever.

In general  $u$  varies periodically between  $u_1$  and  $u_2$ . In Fig. 5 (bottom panel) we plot  $\dot{u}$ , given by (75), against  $u$  for the case  $\mathcal{J} = 0$  for a range of values of  $E$ . Each curve represents the projection of the trajectory of the modulation envelope for a particular energy. The centre at  $u = \frac{1}{3}$  has unchanging  $u$  and corresponds to the cup-like and cap-like solutions of §3.1. The outermost contour is the solution for  $E = 0$ , given by (78).

The general solution of (76) may be found in terms of Jacobian elliptic functions. We introduce a new dependent variable

$$w = \sqrt{\frac{u - u_1}{u_2 - u_1}}$$

and the equation takes the standard form

$$\left(\frac{dw}{d\tau}\right)^2 = \nu^2(1 - w^2)(1 - k^2w^2) \quad (79)$$

where  $\nu^2 = (u_3 - u_1)/4$  and  $k^2 = (u_2 - u_1)/(u_3 - u_1)$ . The general solution of (79) is  $w = \text{sn}[\nu(\tau - \tau_0)]$ , an elliptic function of modulus  $k$ , so that

$$u = u_1 + (u_2 - u_1) \text{sn}^2[\nu(\tau - \tau_0)] \quad (80)$$

The function  $\text{sn } \theta$  has period  $4K$  where  $K$  is the complete elliptic integral:

$$K = K(k) = \int_0^1 \frac{dw}{\sqrt{(1-w^2)(1-k^2w^2)}}. \quad (81)$$

The square of this function (and therefore  $u$ ) has period  $2K$ . The oscillation amplitudes are given by

$$C = \frac{1}{2}N \left( u_1 + (u_2 - u_1) \text{sn}^2[\nu\kappa N(t - t_0)] \right)^{1/2} \quad (82)$$

$$S = N \left( (1 - u_2) + (u_2 - u_1) \text{cn}^2[\nu\kappa N(t - t_0)] \right)^{1/2} \quad (83)$$

and they vary with period  $T = 2K/\nu\kappa N$ .

In the special case  $E = 0$  and  $\mathcal{J} = 0$ , we have  $u_1 = 0$  and  $u_2 = u_3 = 1$  so that  $\nu = \frac{1}{2}$  and  $k = 1$ . In this limit  $\text{sn } x = \tanh x$  and  $\text{cn } x = \text{sech } x$ , and we recover the solution (78). In case  $u_2 = u_1$ , both  $C$  and  $S$  are constant; there is no modulation of the oscillations and no energy exchange between swinging and springing components. These are the special solutions discussed in §3.2.

## 6 Precession of the Swing Plane

There is a particular feature of the behaviour of the physical spring which is fascinating to watch. The bob cannot pass below the point of suspension unless the angular momentum vanishes. However, if the horizontal projection of the motion is an ellipse of high eccentricity, the motion appears to be planar. We may call the vertical plane through the major axis the *swing plane*. When started with almost vertical springing motion, the movement gradually develops into an essentially horizontal swinging motion. This does not persist, but is soon replaced by springy oscillations similar to the initial motion. Again a horizontal swing develops, but now in a different direction. This variation between springy and swingy motion continues indefinitely. The change in direction of the swing plane from one horizontal excursion to the next is difficult to predict: the plane of swing precesses in a manner which is quite sensitive to the initial conditions.

A full knowledge of the solution of (68)–(73) would suffice to determine the swing plane. However, it appears difficult to derive explicit solutions for all the slow variables. In this section, we apply a perturbation technique to the equations expressed in rotating co-ordinates, and derive a solution for the slow rotation of the swing plane. It will be shown to reduce in particular cases to solutions already obtained. The approximate solutions will be compared to numerical solutions of the general system (3)–(5) and will be seen to portray the behaviour of the motion realistically.

## 6.1 Modulation Equations in Rotating Co-ordinates

Once again, we will consider the motion as having aspects with both fast and slow time scales, and apply two-timing. We consider the small-amplitude equations in axes  $(\xi, \eta, \zeta)$  which rotate with angular velocity  $\dot{\Theta}(t) = \Omega(t)$  about the vertical:

$$\ddot{\xi} + (\omega_R^2 - \Omega^2)\xi - 2\Omega\dot{\eta} - \eta\ddot{\Theta} = \lambda\xi\zeta$$

$$\ddot{\eta} + (\omega_R^2 - \Omega^2)\eta + 2\Omega\dot{\xi} + \xi\ddot{\Theta} = \lambda\eta\zeta$$

$$\ddot{\zeta} + 4\omega_R^2\zeta = \frac{1}{2}\lambda(\xi^2 + \eta^2)$$

We seek solutions for which the motion is elliptical in the  $\xi$ – $\eta$ -plane, with axes which may vary slowly:

$$\xi = \epsilon A(t_1) \cos(\omega(t_1)t_0) + \epsilon^2 \xi_2(t_0, t_1) + \dots$$

$$\eta = \epsilon B(t_1) \sin(\omega(t_1)t_0) + \epsilon^2 \eta_2(t_0, t_1) + \dots$$

$$\zeta = \epsilon C(t_1) \cos(2\omega(t_1)t_0 + \gamma(t_1)) + \epsilon^2 \zeta_2(t_0, t_1) + \dots$$

(Note that  $A$ ,  $B$  and  $\gamma$  have different meanings here than in the previous sub-section.) It will transpire that the centrifugal terms (with  $\Omega^2$ ) and the Euler terms (with  $\ddot{\Theta}$ ) do not enter until the third order in  $\epsilon$ . The frequency is assumed to consist of a constant part and a smaller part which may vary slowly,

$$\omega = \omega_0 + \epsilon\omega_1(t_1) + \dots,$$

and the rotation of co-ordinates is also assumed to be small,  $\Omega = \epsilon\Omega_1(t_1)$ . The first order perturbation equations require  $\omega_0 = \omega_R$ . The second-order equations can then be written:

$$(D_0^2 + \omega_0^2)\xi_2 = 2\omega_0[D_1 A \sin \omega t_0 + (\omega_1 A + \Omega_1 B) \cos \omega t_0] + \lambda A C \cos \omega t_0 \cos(2\omega t_0 + \gamma)$$

$$\begin{aligned}
(D_0^2 + \omega_0^2)\eta_2 &= 2\omega_0[-D_1B \cos \omega t_0 + (\Omega_1A + \omega_1B) \sin \omega t_0] + \lambda BC \sin \omega t_0 \cos(2\omega t_0 + \gamma) \\
(D_0^2 + 4\omega_0^2)\zeta_2 &= 4\omega_0[(CD_1\gamma + 2\omega_1C) \cos(2\omega t_0 + \gamma) + D_1C \sin(2\omega t_0 + \gamma)] \\
&\quad + \frac{1}{2}\lambda[A^2 \cos^2 \omega t_0 + B^2 \sin^2 \omega t_0]
\end{aligned}$$

At this order, we can replace  $\omega_0^2$  by  $\omega^2$  on the left sides, so  $\omega$  is the relevant frequency for resonance. As usual, we require secular terms in the second-order equations to vanish. Separation of the coefficients multiplying  $\cos \omega t_0$  and  $\sin \omega t_0$  then yields six equations for six unknowns ( $A, B, C, \gamma, \omega_1, \Omega_1$ ). We write  $\dot{A} = D_1A$ , etc., so that dots now denote derivatives with the slow time, and define  $\kappa = \lambda/4\omega_0 = \lambda/4\omega_R$ , as before. The equations may then be written:

$$\dot{A} = \kappa AC \sin \gamma \quad (84)$$

$$\dot{B} = -\kappa BC \sin \gamma \quad (85)$$

$$\dot{C} = -\frac{1}{4}\kappa(A^2 - B^2) \sin \gamma \quad (86)$$

$$C(\dot{\gamma} + 2\omega_1) = -\frac{1}{4}\kappa(A^2 - B^2) \cos \gamma \quad (87)$$

$$\omega_1 = -\kappa[(A^2 + B^2)/(A^2 - B^2)]C \cos \gamma \quad (88)$$

$$\Omega_1 = \kappa[2AB/(A^2 - B^2)]C \cos \gamma \quad (89)$$

These are the basic modulation equations which we will examine.

It is easily shown that there are three constants of the motion:

$$N^2 = A^2 + B^2 + 4C^2$$

$$H = (A^2 - B^2)C \cos \gamma$$

$$J = AB.$$

We may also show, by squaring (86) and using these constants, that the equation for  $C$  is identical in form to (74) derived in the previous section (as it must be, since the co-ordinate rotation does not affect the vertical motion). Thus, the solution for  $C$  is again given by (82). Using the constants of the motion in (89), the precession rate can be written

$$\boxed{\Omega_1 = \frac{2\kappa JH}{(N^2 - 4C^2)^2 - 4J^2}} \quad (90)$$

Thus, once  $C$  is known,  $\Omega_1$  can be computed immediately. The precession angle  $\Theta$  can then be ascertained by integrating  $\Omega_1$  over the time interval of the motion.

An equation for  $\gamma$  in terms of  $C$  is derived by eliminating  $\omega_1$  from (87):

$$\dot{\gamma} = \kappa \left\{ \left( \frac{2(N^2 - 4C^2)}{H} \right) C^2 \cos^2 \gamma - \frac{H}{4C^2} \right\}$$

This can be solved by quadrature, giving  $t$  as a function of  $\gamma$  and the solution inverted (in principle) to yield  $\gamma$ . Then (84) and (85) give  $A$  and  $B$  and the angular velocity  $\omega_1$  follows from (88).

We look at two special cases where the solutions are particularly simple. First, let us suppose that  $\gamma \equiv 0$ . Then  $A$ ,  $B$  and  $C$  are constants. The modulation equations imply

$$2\omega_1 C = -\frac{1}{4}\kappa(A^2 - B^2) \quad (91)$$

$$\omega_1 = -\kappa[(A^2 + B^2)/(A^2 - B^2)]C \quad (92)$$

$$\Omega_1 = \kappa[2AB/(A^2 - B^2)]C \quad (93)$$

which lead immediately to the solutions for unmodulated elliptic-parabolic motion already obtained in §3.2 above (equations 37–39).

The second special case is for  $\gamma \equiv \pi/2$ . This means  $H = 0$ ,  $\omega_1 = 0$  and  $\Omega_1 = 0$  and the modulation equations become

$$\dot{A} = \kappa AC, \quad \dot{B} = -\kappa BC, \quad \dot{C} = -\frac{1}{4}\kappa(A^2 - B^2). \quad (94)$$

The exact solution for  $C$  follows as a special case of (82) with  $u_1 = 0$ :

$$C = \frac{1}{2}N\sqrt{1 - 2|J|/N^2} \operatorname{sn}[\nu\kappa N(t - t_0)]. \quad (95)$$

Exact solutions for  $A$  and  $B$  may now be derived from (94), but it is more revealing to consider approximate expressions. We seek a solution of the form  $C = C_0 \cos \nu t$ . Since  $\dot{C}(0) = 0$ , it follows that  $A_0 = \pm B_0$ . Supposing now that  $|C_0/A_0| \ll 1$ , it is easy to show (consider  $\ddot{C}(0)$ ) that  $\nu = \kappa A_0$ , and approximate solutions for  $A$  and  $B$  follow:

$$A = A_0 + C_0 \sin \kappa A_0 t$$

$$B = A_0 - C_0 \sin \kappa A_0 t.$$

These solutions correspond to the near-conical solutions considered in §4.

## 6.2 Approximation of the Precession Angle

It is possible to derive an approximate expression for the precession of the swing plane. The total precession angle is simply the time integral of  $\Omega$  (we drop the subscript on  $\Omega_1$ ).

Thus, if the modulation period is  $T$ , the angle through which the major axis precesses in one modulation cycle is

$$\Delta\Theta(t) = \int_{-T/2}^{T/2} \Omega(t) dt. \quad (96)$$

What we desire is an expression for  $\Delta\Theta$  in terms of the initial conditions. If we write (89) in the form

$$\Omega = \frac{2\kappa J}{H} (C \cos \gamma)^2 \quad (97)$$

it is clear that  $\Omega$  is large when  $C \cos \gamma$  is large and small when the latter is small. Let us assume initial conditions such that  $C(0) = C_0$  is at a maximum and  $\gamma(0) = 0$ . Guided by numerical evidence, we seek a solution

$$\Omega = \Omega_0 \operatorname{sech}^2 \mu t \quad (98)$$

where  $\Omega_0 = 2\kappa J C_0^2 / H$  and  $\mu$  must be found. Since  $\operatorname{sech}^2 \mu t$  falls off rapidly for large argument, the precession angle may be estimated as follows:

$$\Delta\Theta \approx \int_{-\infty}^{+\infty} \Omega_0 \operatorname{sech}^2 \mu t dt = \frac{2\Omega_0}{\mu}. \quad (99)$$

As we are interested in the solution near  $t = 0$  we may assume, to a first approximation, that  $C$  remains constant. Combining (97) and (98) we easily show that

$$C \cos \gamma = C_0 \operatorname{sech} \mu t, \quad C \sin \gamma = C_0 \tanh \mu t. \quad (100)$$

The latter implies  $\mu = \dot{\gamma}(0)$ . However, assuming  $|A_0^2 - B_0^2| \ll C_0^2$ , we can neglect the right-hand side of (87); then using (88) and (89), we have

$$\dot{\gamma}(0) = \frac{A_0^2 + B_0^2}{A_0 B_0} \Omega_0.$$

Substituting this in (99), we arrive at

$$\Delta\Theta = \frac{2A_0 B_0}{A_0^2 + B_0^2}. \quad (101)$$

This is the form we want: given the initial amplitudes  $A_0$  and  $B_0$ , and under the assumptions made, we have an approximate expression for the precession angle. Note that  $\Delta\Theta$  depends only on the ratio  $B_0/A_0$ , or effectively on the initial eccentricity and not on the absolute sizes of  $A_0$  and  $B_0$ .

### 6.3 A Numerical Example

We compare the results of numerical integrations of the exact equations (3)–(5) and the approximate modulation equations for small amplitude motions, (84)–(89). We will see that the modulation equations provide a good description of the low-frequency envelope of the motion.

The initial conditions are set as follows:

$$(x_0, y_0, z_0) = (0.04, 0, 0.08); \quad (\dot{x}_0, \dot{y}_0, \dot{z}_0) = (0, 0.03427, 0).$$

The corresponding initial values for the modulation equations are given by

$$A_0 = x_0, \quad B_0 = \dot{y}_0/\omega_R, \quad C_0 = z_0, \quad \gamma_0 = 0.$$

The constants of the motion take the following values:

$$N^2 = 0.027319, \quad H = 0.00011848, \quad J = 0.00043636.$$

The roots of the equation  $E - V = 0$  are then  $(u_1, u_2, u_3) = (0.0013822, 0.95031, 1.0483)$ . Thus  $\nu = \sqrt{(u_3 - u_1)/4} = 0.51160$  and  $k^2 = (u_2 - u_1)/(u_3 - u_1) = 0.90639$ . We calculate  $K$  from the convergent series ([3], p345)

$$K(k) = \frac{\pi}{2} \left\{ 1 + \sum_{n=1}^{\infty} \left( \frac{1 \cdot 3 \cdot 5 \cdots (2n-1)}{2 \cdot 4 \cdot 6 \cdots 2n} \right)^2 k^{2n} \right\}$$

truncated at the required accuracy, and find  $K = 2.6092$ . Then the modulation period predicted by the perturbation analysis is

$$T = \frac{2K}{\nu \kappa N} = 26.2 \text{ seconds}.$$

We shall see that the period of the numerical solution is about 25 seconds, quite close to the value predicted by this formula.

In Fig. 6(a) we plot  $R = \sqrt{x^2 + y^2}$  versus time for the exact solution. Also plotted are  $A$  and  $B$ , the minimum and maximum of the modulation envelope. We see that these curves closely follow the extreme values of the full solution. During the integration time of 150 seconds there are six horizontal excursions, so the modulation period is about 25 s. In Fig. 6(b) we plot  $z$  versus time for the exact solution and also the function  $C$ . Again, the modulation envelope of the vertical component, calculated from (86), closely follows the extrema of the exact solution.

In Fig. 7(a) we plot  $y$  vs.  $x$  for the exact solution. The precession angle between horizontal excursions is  $30^\circ$  (the value of  $\dot{y}_0$  was tweaked to tune the precession angle to an even fraction of  $360^\circ$ ). Thus, the major axis passes through  $180^\circ$  in 150 seconds. It may be noted that many beautiful patterns may be generated by plotting solutions of the spring equations with varying parameters.

The azimuthal angle  $\vartheta$  of the numerical solution of the exact equations may be estimated by averaging the solution over a fast period  $\tau_R$  and considering the mean maximum and minimum values  $R_A$  and  $R_B$ . Then  $\vartheta = \arctan(R_B/R_A)$ . This is compared in Fig. 7(b) to the corresponding value  $\Theta$  resulting from integration of the modulation equation (90). It is noteworthy that  $\vartheta$  and  $\Theta$  remain quasi-constant for most of the modulation cycle, changing rapidly over short intervals around the times when  $C$  is maximum (and  $A^2 - B^2$  is minimum). We see that the solution of the modulation equations advances in phase slightly faster than the exact solution — about  $1\frac{1}{3}^\circ$  per modulation cycle — but the character of the solution for  $\Theta$  is very similar to that of  $\vartheta$ .

The azimuthal change between successive horizontal excursions is very close to  $30^\circ$  for the exact solution. The formula (101) derived in the previous section gives a value

$$\Delta\Theta = \frac{2A_0B_0}{A_0^2 + B_0^2} = 29.1^\circ.$$

It is approximately correct; the small discrepancy is not surprising, considering the various assumptions which were necessary to derive the approximate formula.

The accuracy of the predicted precession angle using (101) is fortuitous. The numerical solution was re-calculated with all parameters unchanged except that  $\dot{y}_0$  was set so that  $B_0 = 0.95A_0$ . The integration was extended for 43 sec., about twice the modulation period. In Fig. 8(a) we plot the horizontal projection of the solution, and in Fig. 8(b) the values of  $\vartheta$  and  $\Theta$  (as in Fig. 7(b)). It is clear that the precession angle is close to  $90^\circ$ . If we repeat the analysis of the preceding section, but seek an approximate solution of the form

$$\Omega = \frac{\Omega_0}{1 + (t/\tau)^2},$$

a so-called Versiera or Witch of Agnesi form ([3], p729) instead of the ‘sech-squared’ form, we find that  $\tau = 1/\dot{\gamma}(0)$  and it follows that

$$\Delta\Theta = \frac{\pi A_0 B_0}{A_0^2 + B_0^2}. \quad (102)$$

The formula (101) gives the result  $\Delta\Theta = 57.22^\circ$  in this case, whereas (102) give the value  $\Delta\Theta = 89.88^\circ$ . It appears that (101) gives good results for small  $B_0/A_0$  while (102) is more accurate for  $B_0 \approx A_0$ , giving the correct limit  $\pi/2$  as  $B_0/A_0 \rightarrow 1$ . It would be more satisfactory to derive a uniform approximation, which would predict the precession rate for arbitrary values of  $B_0/A_0$ . It is hoped to address this problem in another paper.

Finally, we note that, if the initial motion is quasi-vertical, both  $A_0$  and  $B_0$  are minute, and their ratio cannot be determined accurately. Thus, the precession angle cannot be predicted with any precision.

## 7 Summary

A perturbation analysis of the motion of the elastic pendulum or swinging spring in three dimensions has been carried out. The resonance phenomenon, found when the ratio of the elastic and pendular frequencies is 2:1, was studied. For small amplitude motion, the Lagrangian was approximated by keeping terms up to cubic order: the system then has three independent constants of motion and is completely integrable. The linear modes of the system were derived, and simple conical motion was studied. Periodic and quasi-periodic solutions were found, which generalize the solutions first found by Vitt and Gorelik [21]. A two-timing perturbation technique was applied: the motion was assumed to comprise fast oscillations modulated by a low-frequency envelope. Perturbations about conical motion were describable in terms of elementary functions. Then the full perturbation equations were derived. The amplitude of the vertical component was solved in terms of elliptic functions. To solve for the remaining variables it was found to be convenient to base the analysis on the equations in rotating co-ordinates. In this frame, expressions for the precession of the swing-plane were derived. The approximate solutions were compared to numerical integrations of the exact equations, and were found to give a realistic description of the motion.

## Acknowledgements

My thanks to Phil Morrison (Austin), who first drew my attention to the resonance phenomenon for the elastic pendulum. Thanks also to Fergus Larkin (Met Éireann), who sourced a spring and wrought a weight; by curious serendipity, the first weight we tried was precisely that required for resonance, so the spring immediately began to ‘misbehave’. Finally, thanks to Darryl Holm (Los Alamos) for his interest in this work and for his inspiring comments and helpful advice.

## References

- [1] Aničin, B A, D M Davidović and V M Babović, On the linear theory of the elastic pendulum. *Eur. J. Phys.*, **14**, 132–135 (1993).
- [2] Breitenberger, E and R D Mueller, The elastic pendulum: a nonlinear paradigm. *J. Maths. Phys.*, **22**, 1196–1210 (1981).
- [3] Carr, G S, *A Synopsis of Elementary Results in Pure Mathematics*. Francis Hodgson, London, 935pp (1886).
- [4] Carretero-González, R, H N Núñez-Yépez and A L Salas-Brito, Regular and chaotic behaviour in an extensible pendulum. *Eur. J. Phys.*, **15**, 139–148 (1994).
- [5] Cayton, Th E, The laboratory spring-mass oscillator: an example of parametric instability. *Am. J. Phys.*, **45**, 723–732 (1977).
- [6] Cuerno, R, A F Rañada and J J Ruiz-Lorenzo, Deterministic chaos in the elastic pendulum: A simple laboratory for nonlinear dynamics. *Am. J. Phys.*, **60**, 73–79 (1992).
- [7] Davidović, D , B A Aničin and V M Babović, The libration limits of the elastic pendulum. *Am. J. Phys.*, **64**, 338–342 (1996).
- [8] Falk, L, Recurrence effects in the parametric spring pendulum. *Am. J. Phys.*, **46**, 1120–1123 (1978).
- [9] Georgiou, I, On the global geometric structure of the dynamics of the elastic pendulum. *Nonlin. Dynam.*, **18**, 51–68 (1999).
- [10] Heinbockel, J H and R Struble, Resonant oscillations of an extensible pendulum. *J. Appl. Math. Phys.*, **14**, 262–269 (1963).
- [11] Jordan, D W and P Smith, *Nonlinear Ordinary Differential Equations*, 2nd Edn., Oxford Univ. Press, 381pp (1987).
- [12] Kahn, Peter B, *Mathematical Methods for Scientists and Engineers*. John Wiley & Sons, 469pp (1990).
- [13] Kane, T R and M E Kahn, On a class of two-degree-of-freedom oscillations. *J. Appl. Mech.*, **35**, 547–552 (1968).
- [14] Lai, H M, On the recurrence phenomenon of a resonant spring pendulum. *Am. J. Phys.*, **52**, 219–223 (1984).
- [15] Lynch, Peter, The Swinging Spring: a Simple Model for Atmospheric Balance. To appear in *Large-Scale Atmosphere-Ocean Dynamics: Vol II: Geometric Methods and Models*. Cambridge University Press (2001).
- [16] Nayfeh, A H, *Perturbation Methods*. John Wiley & Sons, Inc., 425pp (1973).
- [17] Núñez-Yépez, H N, A L Salas-Brito, C A Vargas and L Vicente, Onset of chaos in an extensible pendulum. *Phys. Lett.*, **A145**, 101–105 (1990).
- [18] Olsson, M G, Why does a mass on a spring sometimes misbehave? *Am. J. Phys.*, **44**, 1211–1212 (1976).
- [19] Rusbridge, M G, Motion of the spring pendulum. *Am. J. Phys.*, **48**, 146–151 (1980).
- [20] Synge, J L and B A Griffith, *Principles of Mechanics*. McGraw-Hill Book Co., 552pp (1959).
- [21] Vitt, A and G Gorelik, Kolebaniya uprugogo mayatnika kak primer kolebaniy dvukh parametricheski svyazannykh lineynykh sistem. *Zh. Tekh. Fiz. (J. Tech. Phys.)* **3**(2-3), 294–307 (1933). Available in English translation: *Oscillations of an Elastic Pendulum as an Example of the Oscillations of Two Parametrically Coupled Linear Systems*. Translated by Lisa Shields, with an Introduction by Peter Lynch. Historical Note No. 3, Met Éireann, Dublin (1999).

### Figure Captions

Fig. 1. A progressive elliptic-parabolic mode. Top: Horizontal projection of the trajectory ( $y$  versus  $x$ ). Bottom: Radial distance plotted against height ( $z$  versus  $R$ ).

Fig. 2. A retrogressive elliptic-parabolic mode. Top: Horizontal projection of the trajectory ( $y$  versus  $x$ ). Bottom: Radial distance plotted against height ( $z$  versus  $R$ ).

Fig. 3. Perturbation of conical motion. Top: Horizontal projection of the trajectory ( $y$  versus  $x$ ). Bottom: Radial distance plotted against height ( $z$  versus  $R$ ).

Fig. 4. Perturbation of conical motion. Top: Radial distance against time ( $R$  versus  $t$ ). Bottom: Eccentricity of horizontal projection.

Fig. 5. Top: Potential energy  $V(u)$  as a function of  $u$  for several values of the angular momentum,  $\mathcal{J} \in \{0, \frac{1}{4}, \frac{1}{2}, \frac{3}{4}, 1\}$ . The horizontal line represents an accessible energy level  $E = -0.025$ . Bottom:  $\dot{u}$  versus  $u$  when  $\mathcal{J} = 0$  for a range of values  $E \in \{-0.073, -0.055, -0.037, -0.018, 0.000\}$ .

Fig. 6. (top) Plot of  $R$  (solid) and  $A$  and  $B$  (dashed) versus time. (bottom) Plot of  $z$  (solid) and  $C$  (dashed) versus time. Initial conditions are given in the text.

Fig. 7. (top) Plot of  $y$  versus  $x$  for the solution of (3)–(5). (bottom) Time evolution of the azimuthal angle  $\vartheta = \arctan(R_B/R_A)$  of the full solution (solid) and  $\Theta$  (dashed) derived from (90). For initial conditions, see the text.

Fig. 8. (top) Plot of  $y$  versus  $x$  for the solution of (3)–(5). (bottom) Time evolution of the azimuthal angle  $\vartheta = \arctan(R_B/R_A)$  of the full solution (solid) and  $\Theta$  (dashed) derived from (90). For initial conditions, see the text.

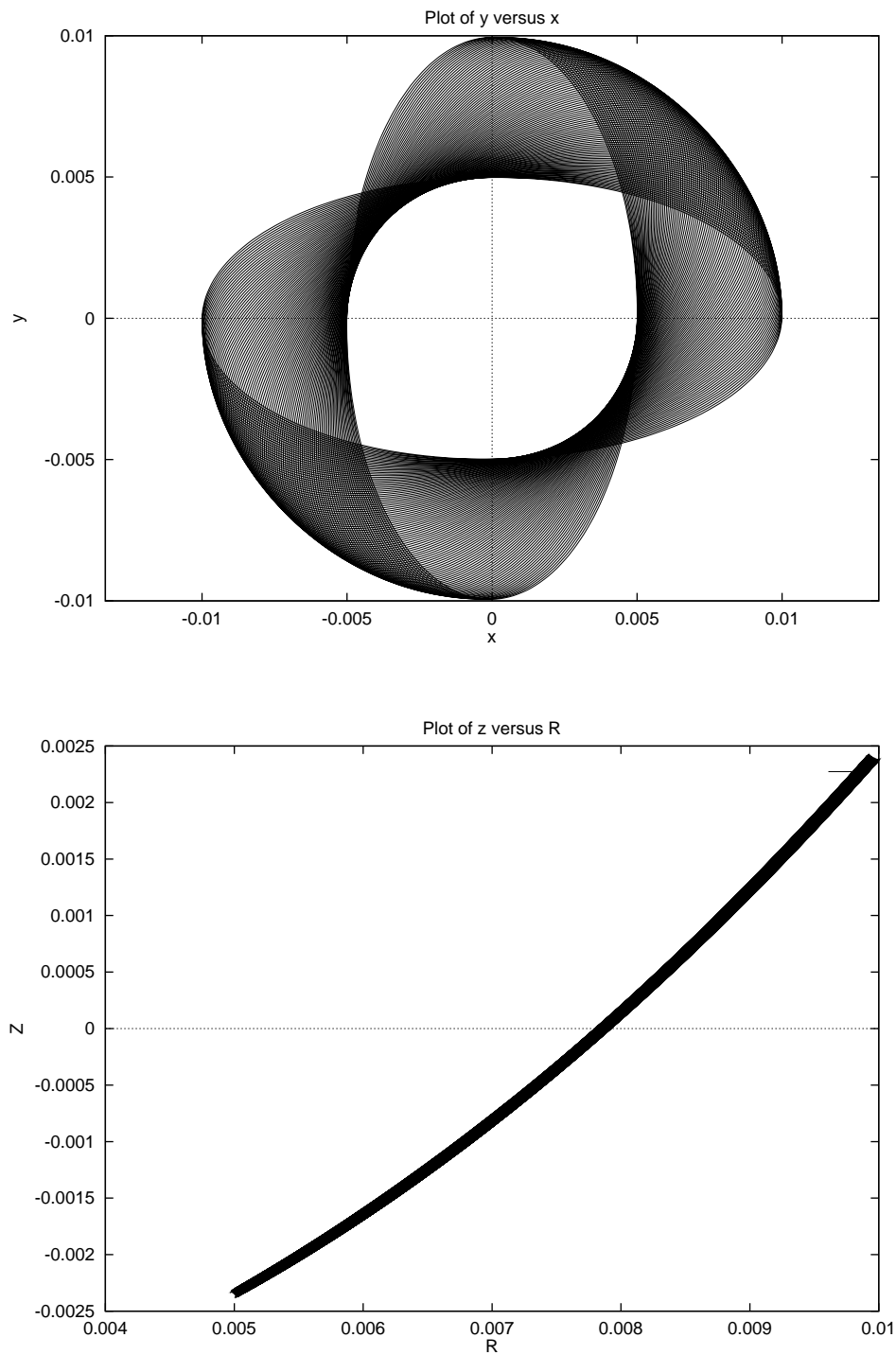


Fig. 1. A progressive elliptic-parabolic mode. Top: Horizontal projection of the trajectory ( $y$  versus  $x$ ). Bottom: Radial distance plotted against height ( $z$  versus  $R$ ).

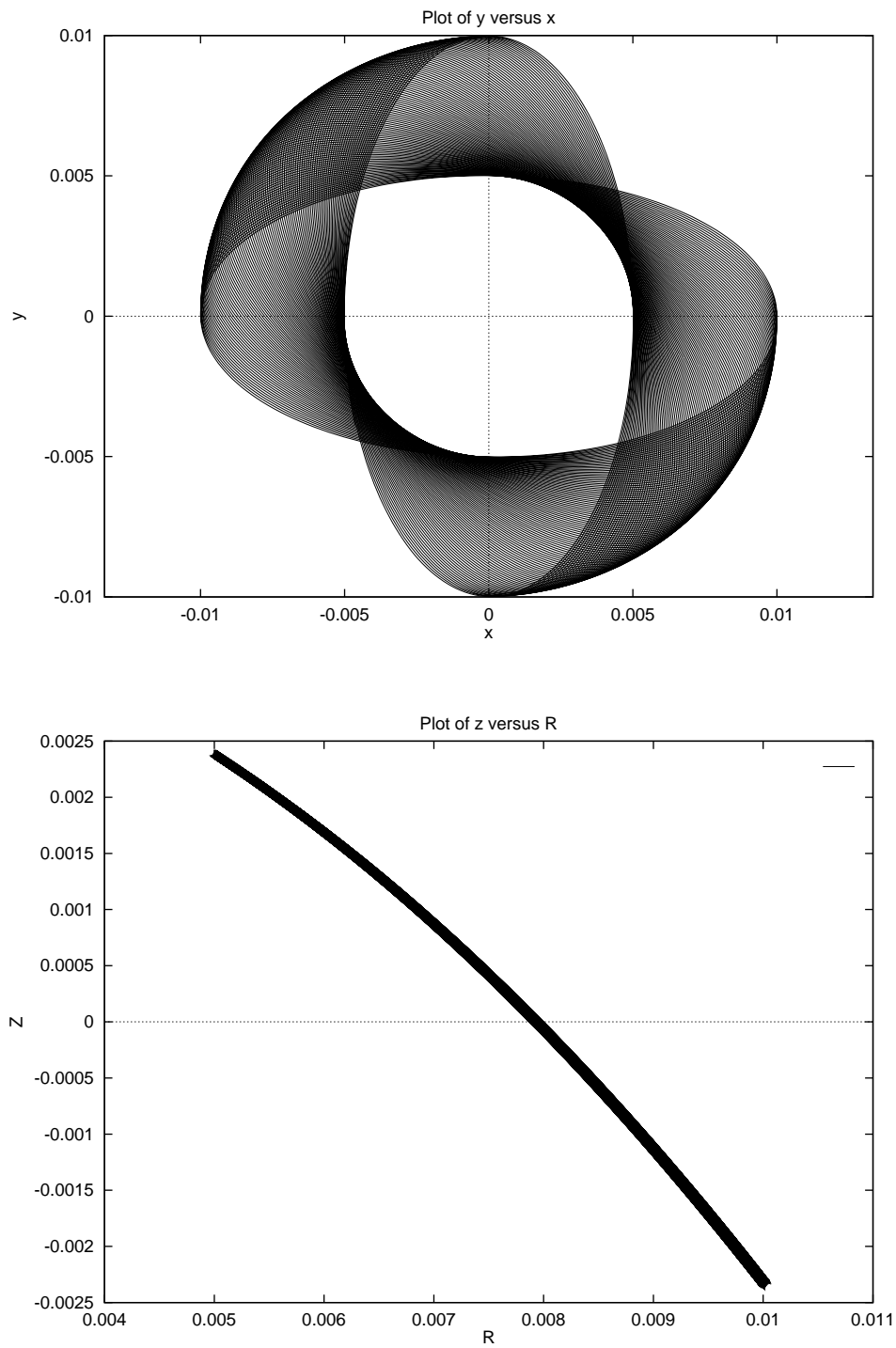


Fig. 2. A retrogressive elliptic-parabolic mode. Top: Horizontal projection of the trajectory ( $y$  versus  $x$ ). Bottom: Radial distance plotted against height ( $z$  versus  $R$ ).

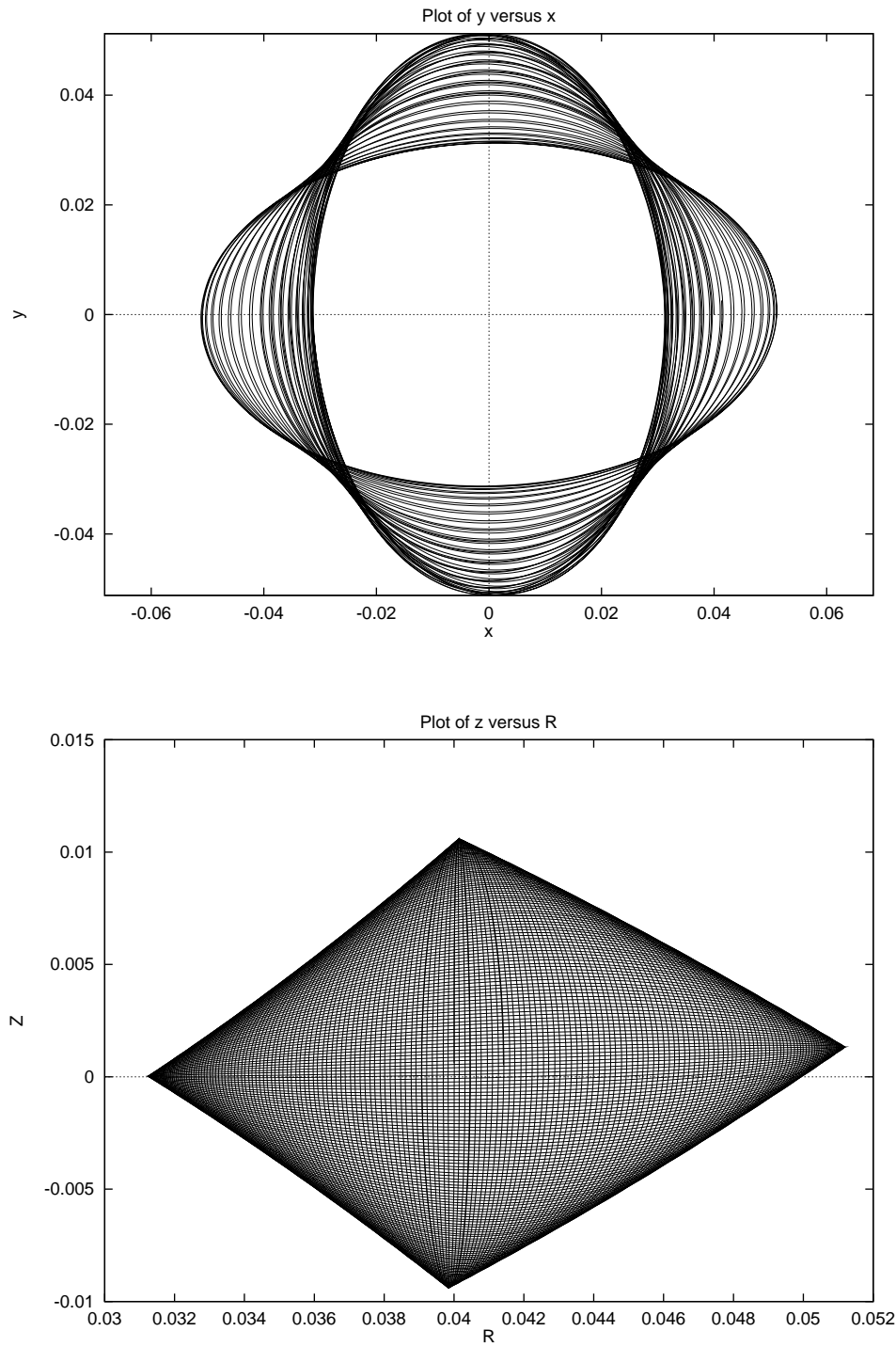


Fig. 3. Perturbation of conical motion. Top: Horizontal projection of the trajectory ( $y$  versus  $x$ ). Bottom: Radial distance plotted against height ( $z$  versus  $R$ ).

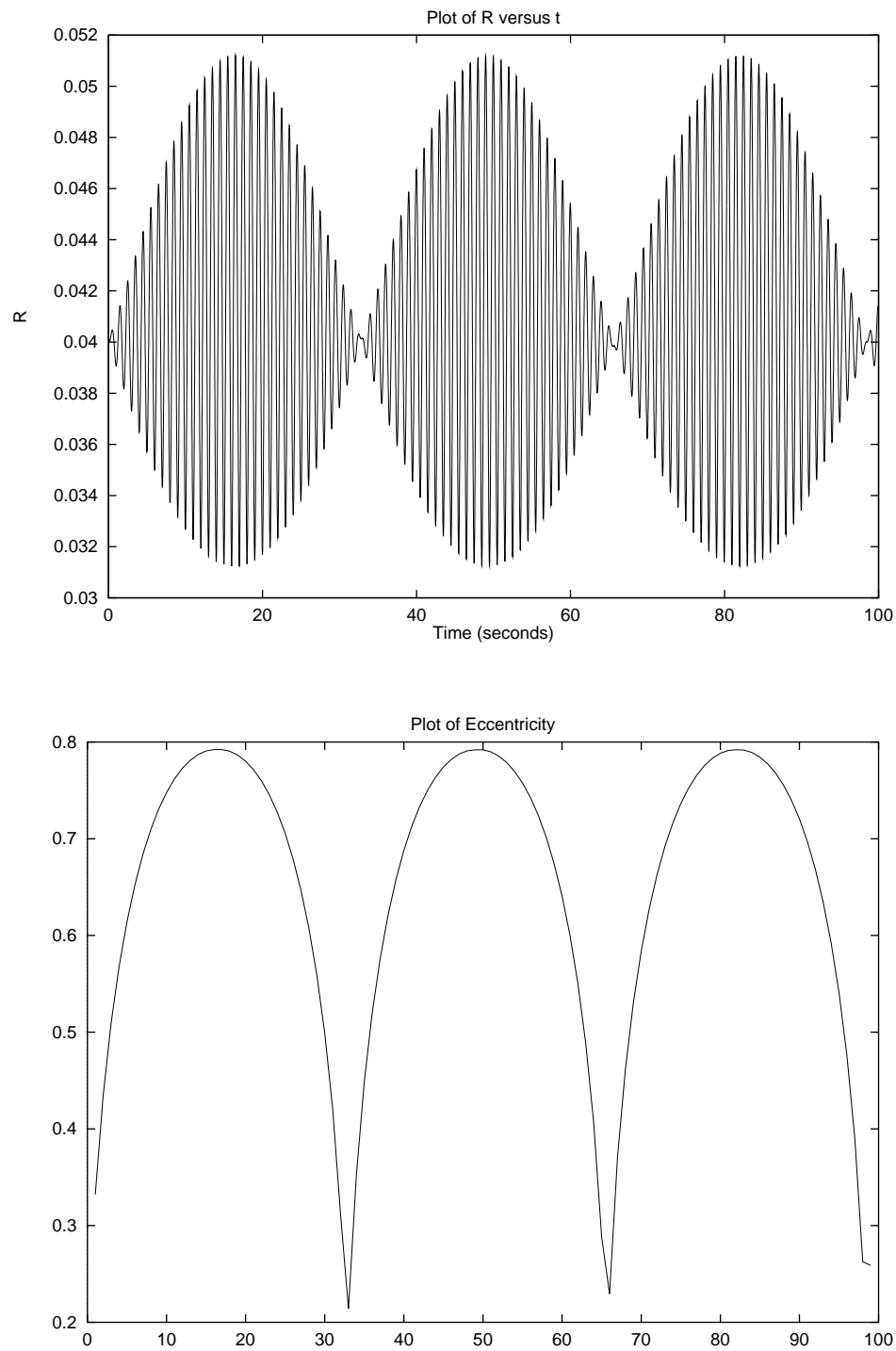


Fig. 4. Perturbation of conical motion. Top: Radial distance against time ( $R$  versus  $t$ ). Bottom: Eccentricity of horizontal projection.

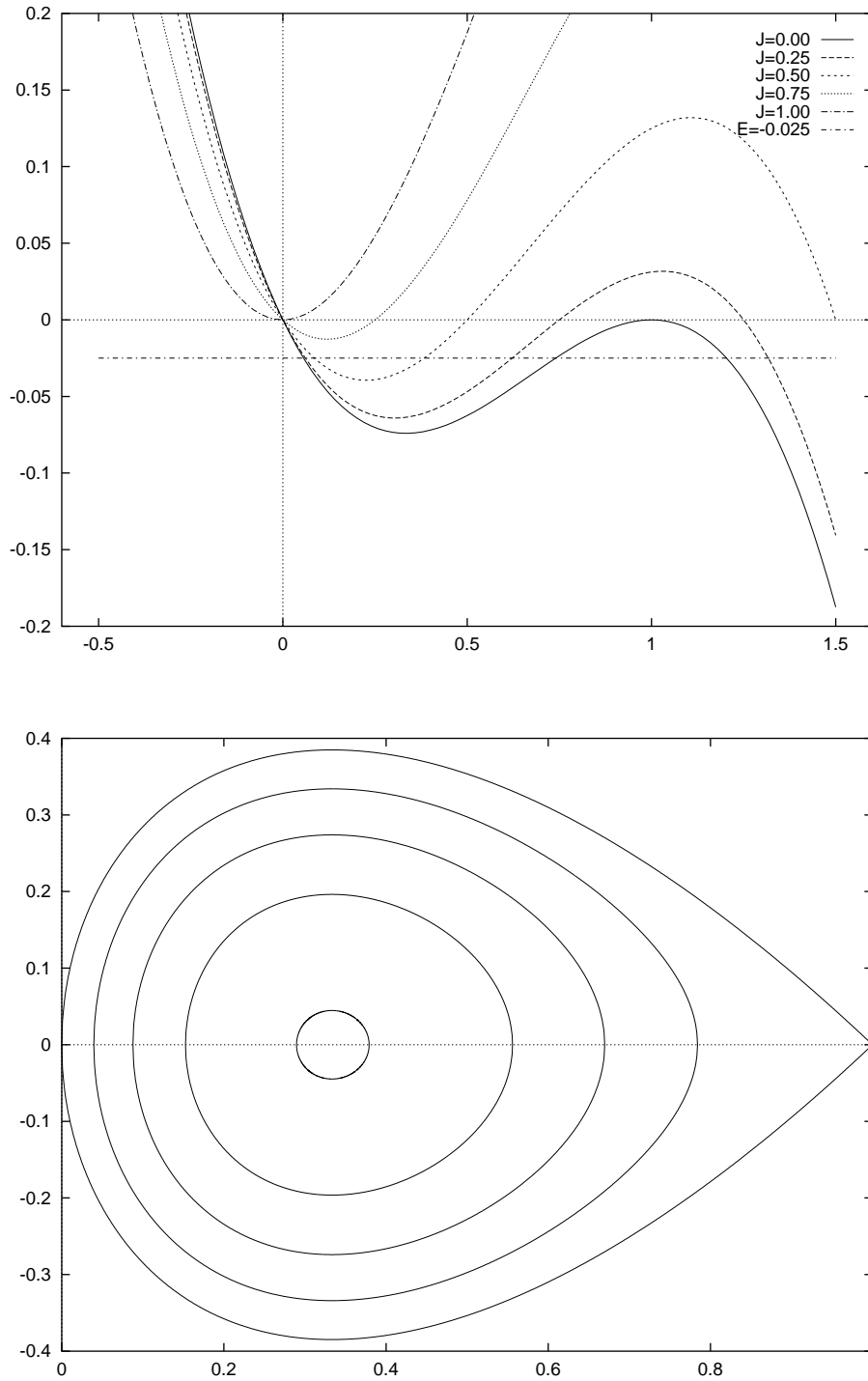


Fig. 5. Top: Potential energy  $V(u)$  as a function of  $u$  for several values of the angular momentum,  $\mathcal{J} \in \{0, \frac{1}{4}, \frac{1}{2}, \frac{3}{4}, 1\}$ . The horizontal line represents an accessible energy level  $E = -0.025$ . Bottom:  $\dot{u}$  versus  $u$  when  $\mathcal{J} = 0$  for a range of values  $E \in \{-0.073, -0.055, -0.037, -0.018, 0.000\}$ .

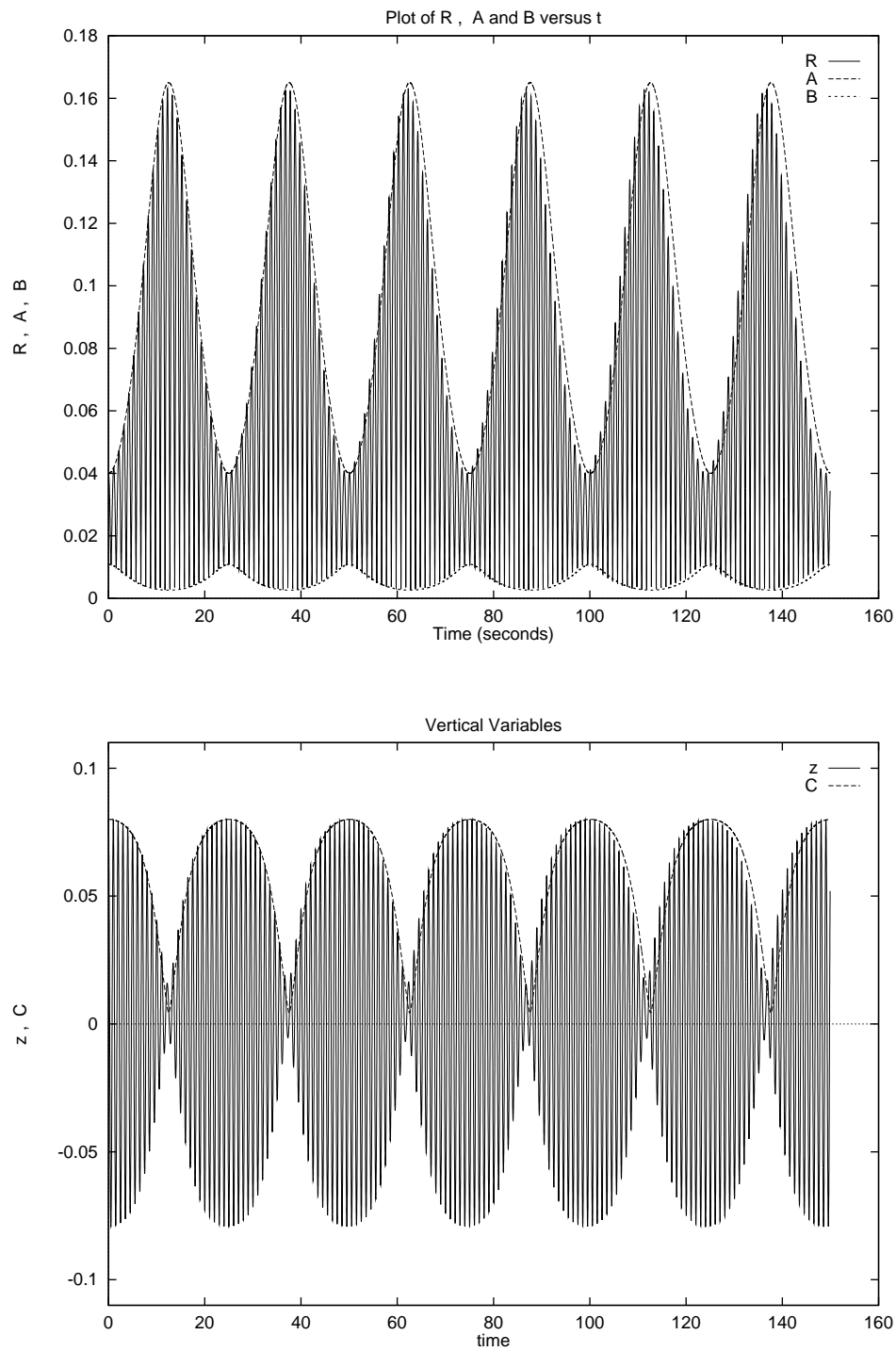


Fig. 6. (top) Plot of  $R$  (solid) and  $A$  and  $B$  (dashed) versus time. (bottom) Plot of  $z$  (solid) and  $C$  (dashed) versus time. Initial conditions are given in the text.

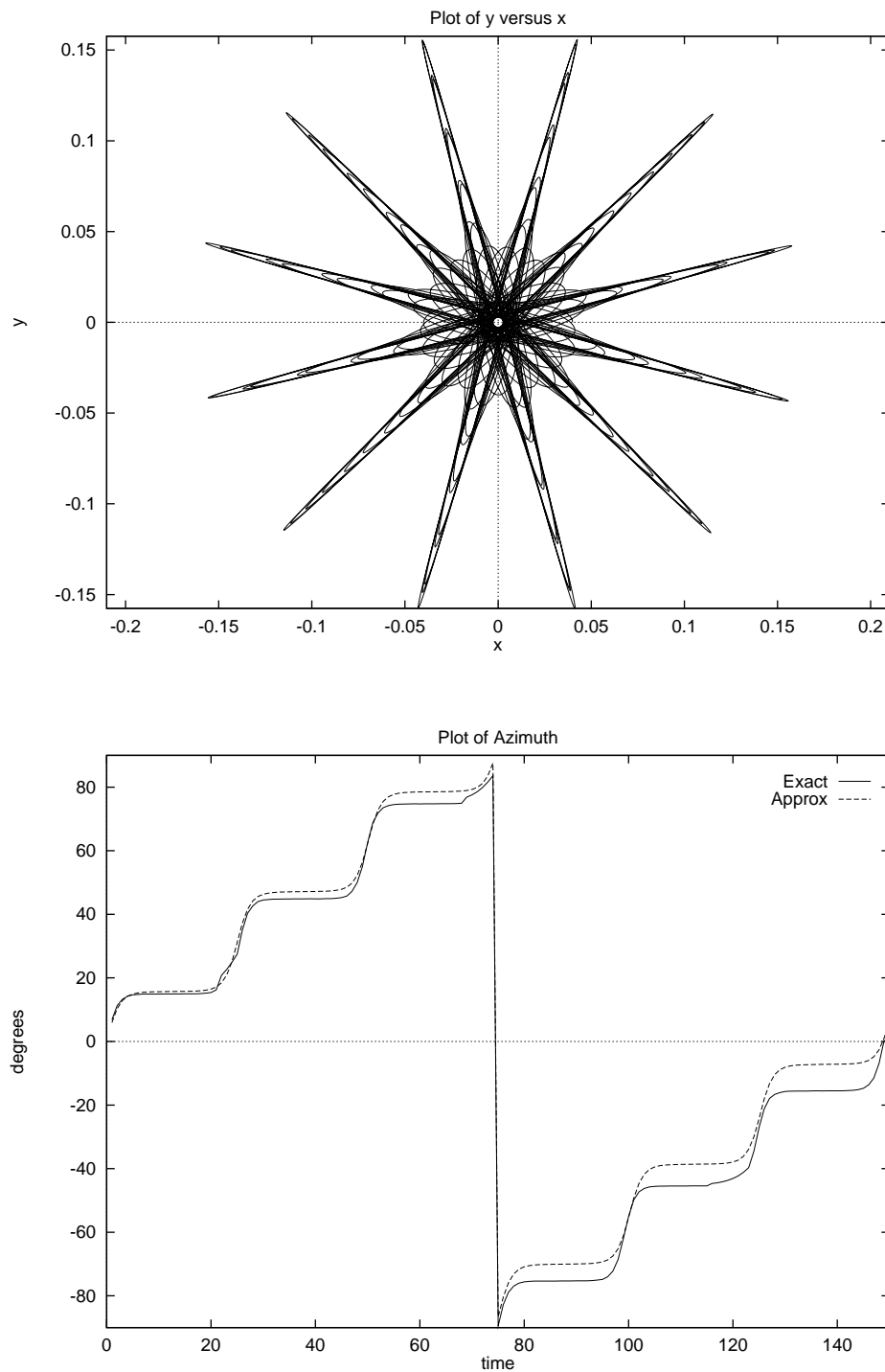


Fig. 7. (top) Plot of  $y$  versus  $x$  for the solution of (3)–(5). (bottom) Time evolution of the azimuthal angle  $\vartheta = \arctan(R_B/R_A)$  of the full solution (solid) and  $\Theta$  (dashed) derived from (90). For initial conditions, see the text.

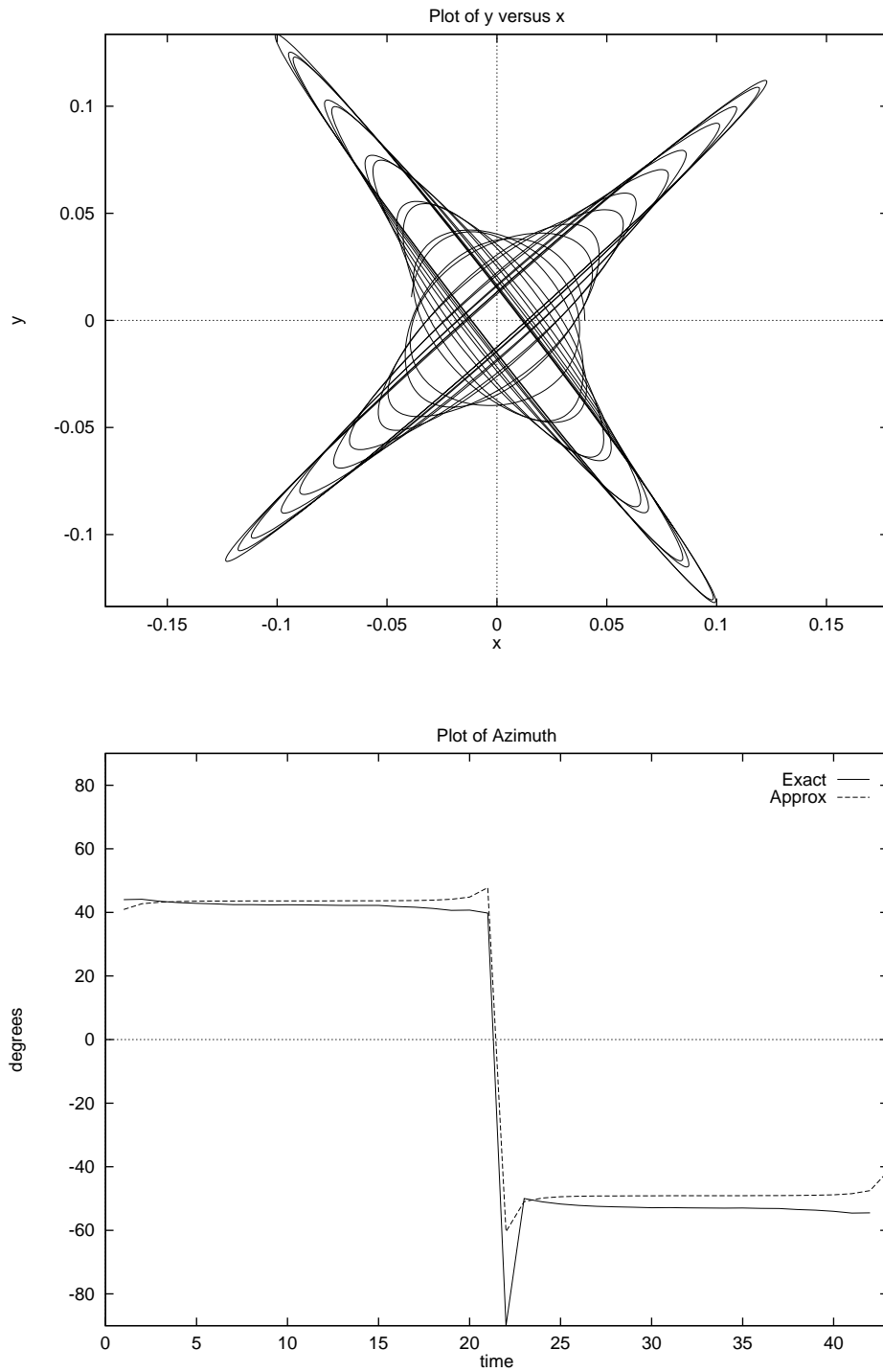


Fig. 8. (top) Plot of  $y$  versus  $x$  for the solution of (3)–(5). (bottom) Time evolution of the azimuthal angle  $\vartheta = \arctan(R_B/R_A)$  of the full solution (solid) and  $\Theta$  (dashed) derived from (90). For initial conditions, see the text.